

# Experimental determination of dynamic and static elastic modulus of high-performance lightweight concrete

Małgorzata Abramowicz<sup>1\*</sup> , Piotr Szewczyk<sup>1\*</sup> , Karol Federowicz<sup>1</sup> 

<sup>1</sup> West Pomeranian University of Technology in Szczecin, al. Piastów 50a, 70-311 Szczecin, Poland

\* Corresponding author's e-mail: mabramowicz@zut.edu.pl, szewczyk@zut.edu.pl

## ABSTRACT

This article focuses on the study of the elastic modulus of modern high-performance lightweight concrete. A characteristic feature of concrete, a brittle and composite material, is that its stress-strain characteristics are not exactly linear. This causes some problems in the definition of the Young's modulus. This paper compares a statically determined modulus, called the secant modulus, with a dynamically determined modulus. The obtained results show that the proportions between static and dynamic moduli are significantly different from the ratios known from the literature for normal concretes. For comparison, the results of similar tests for normal concrete with similar strength properties are presented.

**Keywords:** modulus of elasticity, dynamic analysis, lightweight high-performance concrete.

## INTRODUCTION

### Application of the dynamic module

Concrete is a material with a complex internal structure, which results in a nonlinear stress-strain relationship. The dynamic modulus ( $E_d$ ) of elasticity of concrete is a key parameter widely used in structural engineering, particularly in non-destructive testing (NDT) and monitoring of concrete structures.

It is commonly determined using ultrasonic pulse velocity or vibration-based methods and reflects the material's stiffness under dynamic (rapid or cyclic) loading conditions. In practice,  $E_d$  is often employed to estimate the static modulus of elasticity ( $E_c$ ), which is directly applicable in structural design and analysis—especially when direct testing is impractical or when evaluating in-situ concrete in existing structures [1, 2]

Engineers rely on this methodology in various contexts, such as structural health monitoring, forensic assessments following damage or failure, and in tracking the long-term evolution of material properties caused by factors like moisture changes, aging, freeze-thaw degradation, or

chemical attack [3]. Moreover, the dynamic modulus is used to assess the compressive strength, durability, and overall quality of concrete, as it shows a strong correlation with both compressive strength and the static modulus [4].

When modelling the dynamic behaviour of a composite system—such as a reinforced concrete slab connected to a steel I-beam—the accuracy of the predicted natural frequencies and mode shapes largely depends on the correct specification of material stiffness. In such cases, using the dynamic modulus of elasticity for concrete becomes essential [5].

This parameter plays a critical role in accurately capturing the stiffness distribution within the composite system, which directly influences the predicted dynamic response. In modal analysis, the dynamic modulus affects both global vibrational behaviour and localized deformations, particularly in the concrete slab where stiffness is strain-rate dependent.

In such composite structures, the interaction between concrete and steel elements introduces additional complexity, including shear transfer mechanisms and partial composite action, both

of which are sensitive to the assumed material properties. The dynamic modulus is especially relevant when modelling transient or cyclic loading scenarios, as it better reflects the real-time mechanical response of concrete under such conditions compared to the static modulus.

Furthermore, for finite element simulations or reduced-order models, accurately specifying the dynamic modulus of elasticity allows for improved correlation between numerical predictions and experimental data. This is particularly important in the context of structural retrofitting, damage detection, and the assessment of vibration serviceability in bridges, floor systems, and other infrastructure applications where dynamic performance is critical.

To enhance the accuracy of converting dynamic modulus values to static ones, as well as to predict other mechanical properties relevant for structural calculations, advanced empirical and statistical models have been proposed [6]. Overall, the dynamic modulus of elasticity serves as a critical parameter in non-destructive testing, quality control, and long-term performance evaluation of concrete structures.

### The ratio between the static and dynamic modulus of elasticity

The relationship between the static  $E_c$  and dynamic  $E_d$  modulus of elasticity of concrete has been studied for many years [7–11]. In the great majority of cases, the dynamic modulus achieves values higher than the static modulus. This difference is due to the behaviour of concrete under load and the way these values are defined. Concrete is not a perfectly linear-elastic material. Especially in the first loading cycles, it shows a noticeable non-linearity. Therefore, the normative [12] determination of the modulus takes place after several cycles of stabilising concrete behaviour. The static modulus is determined by a secant line through two points on the stress-strain curve. These points correspond to 10% and 33% of the compressive strength. In this load range, no new cracks are yet developing in the concrete and the material behaviour is closest to linear. The method of determining the dynamic modulus is completely different. This modulus is determined by inducing vibrations on the unloaded element. Thus, the dynamic modulus can be defined by the tangent to the stress-strain curve at zero stress. A tangent defined in this way will have a

greater angle to the strain axis than a secant passing through the two points defined above.

Simple relationships between the dynamic and static modulus of elasticity have been defined many years ago, among e.g. in [13]:

$$E_c = 0.83E_d \quad (1)$$

and British standard [14]:

$$E_c = 1.25E_d - 19 \quad (2)$$

Each of these formulas has its limitations regarding cement content and aggregate type. The authors of formula (2) state that its accuracy should be estimated with a margin of  $\pm 4$  GPa.

For lightweight concretes, in work [15] the following relationship has been proposed:

$$E_c = 1.04E_d - 4.1 \quad (3)$$

For lightweight concretes, differences in modulus of elasticity due to the way the density is reduced can be very pronounced. It may therefore be useful to relate the modulus of elasticity to the material density  $\rho$  [16].

$$E_c = 0.23E_d^{1.4}\rho^{-1} \quad (4)$$

With that said, a factor of 0.23 was adopted by the authors for the imperial unit layout.

However, it is important to bear in mind that the presented relationships were defined many years ago. The development of building materials, including modern concretes, is very dynamic. Currently produced high-performance lightweight concretes (HPLWC) have a much better strength and stiffness to density ratio. Therefore, comprehensive research into the properties of these materials, including dynamic properties, is needed.

## MATERIALS AND METHODS

### Structural concrete

As a reference material, commercial ready-mix concrete used for engineering structures along the S3 expressway in the West Pomeranian Voivodeship was employed. According to the manufacturer's declaration, the concrete was classified as C50/60 in terms of strength and S4 in terms of consistency class. The adopted consistency class, as per the European Standard [17], corresponds to a slump range of 160 mm to 210 mm, characterizing the mixture as flowable.

The concrete mixture exhibited a water-to-cement ratio (w/c) of 0.36 and included natural sand

with a particle size of 0–2 mm and granodiorite aggregate with a grain size of 2–16 mm. In compliance with national standards for bridge concrete, the binder used in the mixture was Portland cement CEM I 42.5R-NA. Rheological and durability properties were ensured by the incorporation of plasticizing and air-entraining admixtures. Laboratory tests confirmed the specified strength class, and additionally, the C50/60 concrete had a density of 2.384 kg/m<sup>3</sup>. Hence, in accordance with the PN-EN 206 standard, it is classified as normal-weight concrete.

### High-performance lightweight concrete

The starting point for designing the lightweight concrete mix was the research conducted by Tahwia et al. [18]. The primary material objective was to achieve a concrete density below 2000 kg/m<sup>3</sup>, qualifying it as lightweight concrete, with a 28-day compressive strength of approximately 60 MPa.

Due to the intended application of the designed lightweight concrete—reinforcing structural elements with thin layers—the mix needed to exhibit high fluidity. Required material has to be flow able without external vibrations and be able to fill voids between reinforcement. Consequently, a self-compacting concrete mix was designed. The binder comprised CEM III/A cement and silica fume, while the aggregate was a blend of quartz powder (filler) and artificial lightweight aggregate (Liaver) with a particle size of up to 0.5 mm. The fluidity and stability of the mix were enhanced using a plasticizing admixture and a shrinkage-reducing agent. The dosage of super plasticiser was 3% of the mass of cement and SRA was 2% of the mass of cement. Glass fibres

with a diameter of 4 mm and a modulus of elasticity of 73 GPa were also used. The detailed composition of the mix is presented in Table 1. The effective water-to-cement ratio was 0.22, and the total water-to-cement ratio was 0.25. The theoretical density was expected to be 1872 kg/m<sup>3</sup>, while the real-life density measured after mixing was 1770 kg/m<sup>3</sup>. The resulting concrete had a density of 1625 kg/m<sup>3</sup> and a compressive strength of 65.93 MPa after 28 days of curing. A full description of the properties of the tested concrete, both fresh and hardened, can be found in [19]. The LS mixture was used in these tests. This mixture was selected for its future application as a strengthening layer material.

### Experimental determination of the static modulus of elasticity

The determination of the secant (static) modulus of elasticity was carried out according to standard [12]. Cylindrical specimens with a diameter of 100 mm and a height of 200 mm were used. The test was carried out on a Zwick/Roell Z600 electromechanical testing machine. Electro-resistance strain gauges with a resistance of 120  $\Omega$  were used to measure strain. At Figure 1a diagram of the location of the strain gauges is shown. Two strain gauges parallel to the specimen axis and two perpendicular to the specimen axis were glued onto each specimen. Pairs of strain gauges were placed opposite each other, creating a scheme similar to an extensometer, eliminating the eventual effect of bending. Each of the four strain gauges was a separate, half-bridge measuring point consisting of a measuring strain gauge and a compensation strain gauge to compensate for any temperature changes during the test (Figure 1a). Figure 1b shows a sample of C50/60 concrete with strain gauges, in Figure 1c sample of HPLWC.

Tests were carried out on days 1, 2, 3, 7, 14 and 28 after concreting. Each time the measurement procedure looked identical and is shown in Figure 2 (example of a C50/60 concrete sample tested after 28 days). Firstly, the compressive strength of the concrete on the day of the test was determined. Three initial load cycles were then carried out between values of 0.5 MPa and a stress corresponding to 10% of the compressive strength  $f_c$ . This was followed by a further 10 loading cycles between 10% and 33% of the compressive strength. Determining the static, secant modulus of elasticity involves measuring the deformation

**Table 1.** Designed high performance light-weight concrete composition

Material	Amount
	kg/m <sup>3</sup>
Cement CEM III 42.5N -LH/HSR/NA	992.5
Silica Fume	157.5
Quartz powder	210.0
Liaver 0.25–0.5 mm	113.3
Liaver 0.1–0.3 mm	84.0
Sika ViscoCrete 3090M	33.3
Chryso serenis	19.8
Glass fiber 4 mm	10.0
Water	251.2

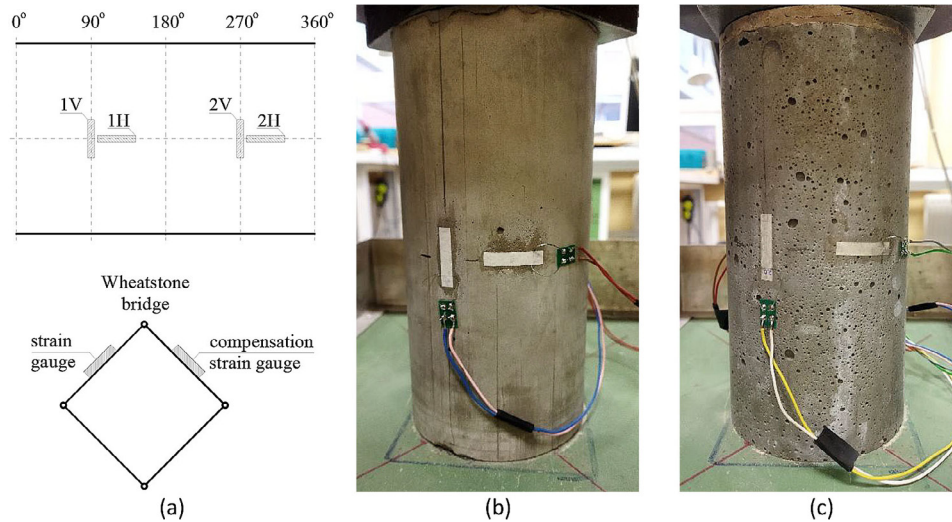


**Figure 1.** Strain measurement using strain gauges, (a) measurement system scheme, (b) C50/60 concrete specimen, (c) HPLWC concrete specimen

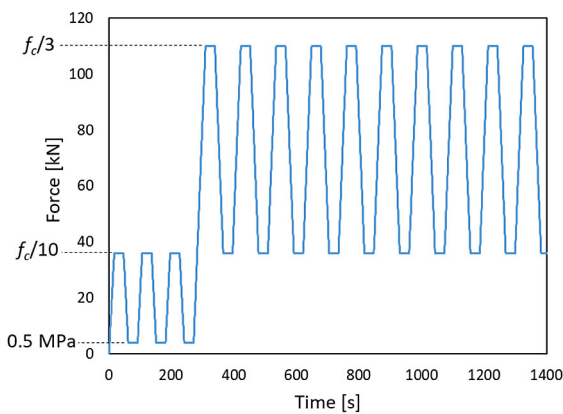


**Figure 2.** Diagram of specimen loading during the test

of concrete over a specified range of stresses. The upper stress limit of 33% of the compressive strength is due to the properties of the concrete. It is assumed that beyond this value, micro-cracks develop in the concrete which causes the stress-strain relationship to become non-linear. An example of the stress-strain relationship is shown in Figure 3 (C50/60 concrete after 28 days).

The concrete shows greater non-linearity in the stress-strain relationship during the first loading cycles, so that the elastic modulus determined from this relationship is underestimated. Normally, stabilisation occurs after 6–7 loading cycles; in this study, 10 cycles were performed for complete stabilisation. According to Hooke's law, the secant modulus of elasticity  $E_c$  is calculated as follows:

$$E_c = \frac{\Delta\sigma}{\Delta\varepsilon} = \frac{\sigma_{fc/3} - \sigma_{fc/10}}{\varepsilon_{fc/3} - \varepsilon_{fc/10}} \quad (5)$$

where:  $\sigma_{fc/3}$  – stress equivalent to 33% of the compressive strength  $f_c$ ;  $\sigma_{fc/10}$  – stress equivalent to 10% of the compressive strength  $f_c$ ;  $\varepsilon_{fc/3}$  – strain equivalent to 33% of the compressive strength  $f_c$ ;  $\varepsilon_{fc/10}$  – strain equivalent to 10% of the compressive strength  $f_c$ .

### Experimental determination of the dynamic modulus of elasticity

For dynamic tests, a different sample shape was used than for static tests. The tests were carried out on prismatic samples (100 × 100 × 400 mm) shown in the Figure 4. An impulse test was performed to determine the dynamic longitudinal modulus of elasticity of the analysed concretes. The dynamic modulus was measured on the same days as for the secant modulus. Tests were conducted on 4 samples of C50/60 concrete and 7 samples of HPLWC. The test involved excitation of the sample's fundamental axial frequency using a KISTLER 9726A20000 modal hammer (Figure 5a). The detailed testing procedure is described in the literature [20, 21], and [22]. During the test, the specimen must remain free to deform longitudinally. To replicate free-free boundary conditions, the sample was suspended on two steel cables (Figure 4), which minimized external damping. The impact was applied to one end of the specimen, and the response was measured on the opposite end using triaxial piezoelectric accelerometers (PCB 356A01, Figure 5b). A steel plate was used at the impact location to reinforce the excitation point and shorten the impulse duration.



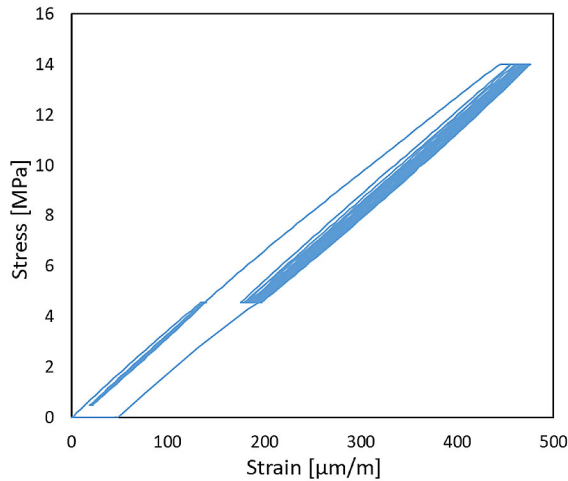


**Figure 3.** Example of stress-strain relationship for one of the tests of C50/60 concrete after 28 days

The sensors used are capable of measuring frequencies from 2 to 8000 Hz in the Y and Z axes, and from 2 to 5000 Hz in the X axis. The sensors were mounted onto the metal surface of the specimen using a dedicated mounting wax. The entire process was recorded using an LMS SCADAS III data acquisition system connected to a computer. Each test consisted of five repeated excitations, and the average fundamental axial frequency was determined using Test.Lab software. As illustrated in Figure 6 and in Figure 7, an example of the amplitude curve of the frequency response function (FRF) recorded during the experimental tests is shown. The data were obtained for Sample 1 made of C50/60 concrete (Figure 6) and Sample 2 made of HPLWC (Figure 7). The graphs exhibit a distinct local peak in the FRF amplitude corresponding to the first resonance frequency. This

frequency represents the fundamental axial vibration mode of the specimen, in which the sample undergoes alternating elongation and contraction.

The speed of waves moving through elastic materials is determined by Newton's formula:

$$v = \sqrt{\frac{E_d}{\rho}} \quad (6)$$

where:  $v$  – speed of wave dispersion [m/s],  $E_d$  – dynamic longitudinal modulus of elasticity of the material [N/m<sup>2</sup>],  $\rho$  – density [kg/m<sup>3</sup>].

Assuming that the speed of wave dispersion and the density of the material can be measured, it is also possible to determine the modulus of elasticity. The propagation velocity of a wave in a sample that oscillates axially in accordance with its fundamental vibration mode is determined by the following relationship:

$$v = f \cdot \lambda \quad (7)$$

where:  $f$  – frequency of vibration [Hz],  $\lambda$  – wavelength [m].

The wavelength is equal to twice the sample length 0.8 m. Following the transformation of Equations 6 and 7, the dynamic longitudinal elastic modulus of the material can be calculated as follows:

$$E_d = (f \cdot \lambda)^2 \cdot \rho \quad (8)$$

Equation 8 indicates that the value of Young's modulus is directly proportional to the vibration frequency and the length of the sample. In order to limit the vibration frequency to ranges measurable by available accelerometers, samples with a

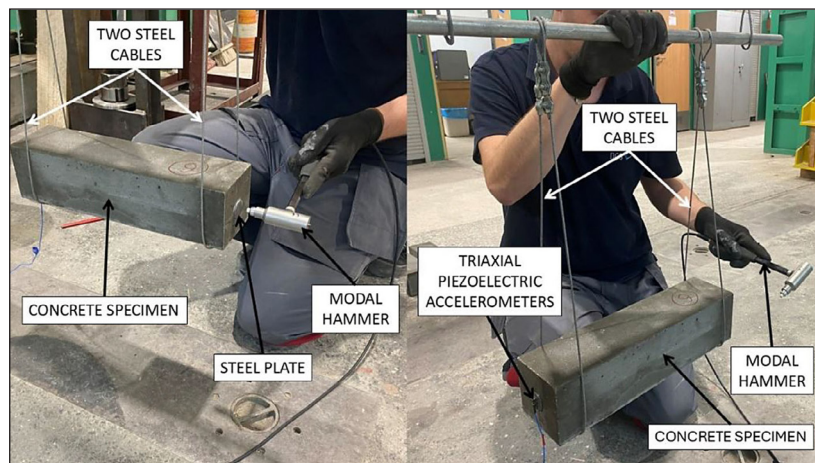


**Figure 4.** Concrete specimen during determination of dynamic modulus: (a) cylindrical (150 × 300 mm), (b) rectangular (100 × 100 × 400 mm)

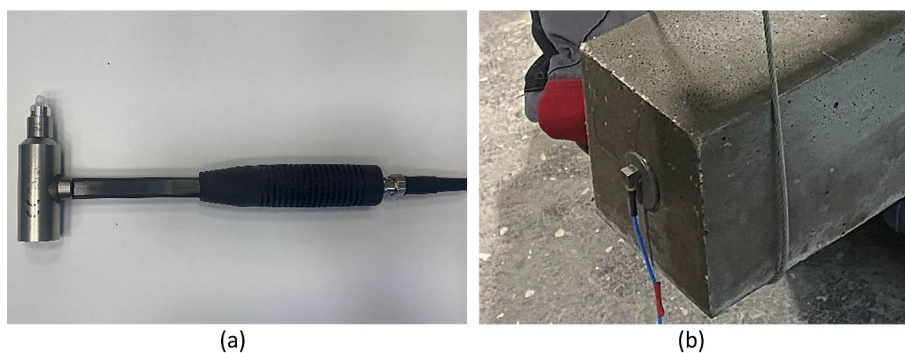


**Figure 5.** Measuring equipment: (a) modal hammer KISTLER 9726A20000, (b) triaxial piezoelectric sensors PCB 356A01

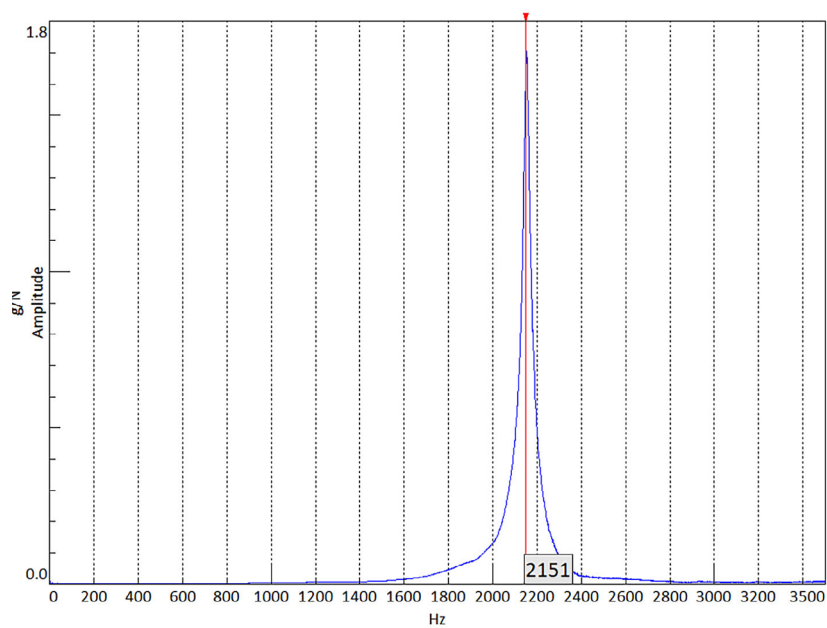


**Figure 6.** FRF amplitude curve for concrete C50/60, sample 1, day 7<sup>th</sup>

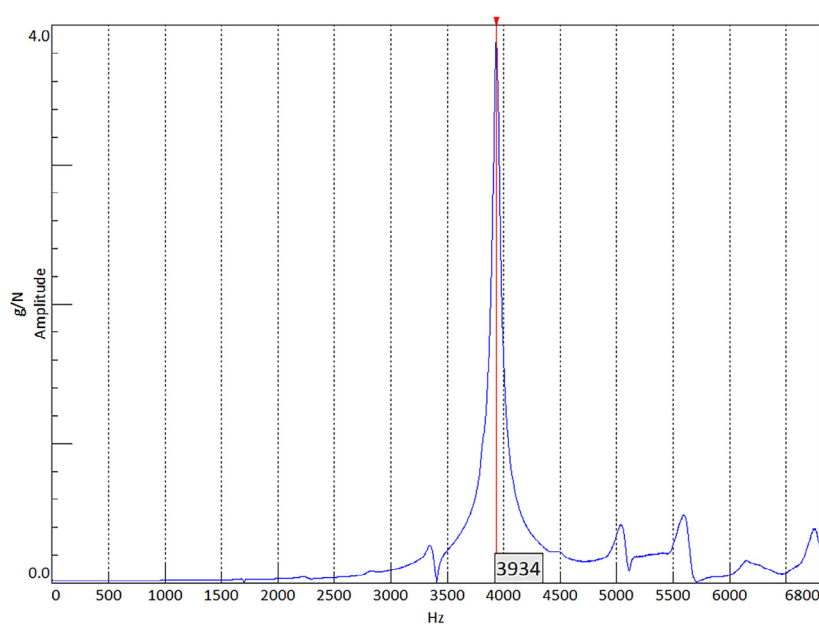


**Figure 7.** FRF amplitude curve for HPLWC, sample 2, day 7<sup>th</sup>

significantly greater length than classic samples for determining the secant modulus were used. The results of these studies are presented in Section 3.2.

## RESULTS AND DISCUSSION

### Static test results

Each time, the determination of the modulus of elasticity was carried out on three specimens. Each of the specimens was subjected to cyclic loading as described in section 2.3. During the last loading cycle, the strains were measured. An example of the results obtained on day 3 of the test is shown below. Table 2 shows the results for concrete C50/60, and Table 3 for HPLWC. The mean values  $\bar{x}$  and standard deviation  $s$  are given

at the end of the tables. The values obtained indicate a high reproducibility of the results.

Figure 8 shows the change in modulus of elasticity over the first 28 days after concreting. Figure 8a shows the results for C50/60, a Figure 8b for HPLWC. Comparing these two graphs shows a clear disparity between the modulus of elasticity of classic structural concrete and lightweight concrete. With a comparable compressive strength value, lightweight concrete has almost half the Young's modulus value of normal concrete.

### Dynamic test results

Testing was carried out on 4 C50/60 concrete samples and 7 HPLWC samples. The smaller number of C50/60 concrete samples was due to the fact that these samples were taken directly on site

**Table 2.** Example  $E_c$  for C50/60 concrete after 3 days after concreting

Sample	$\sigma_{fc/10}$	$\sigma_{fc/3}$	$\Delta\sigma$	$\epsilon_{fc/10}$	$\epsilon_{fc/3}$	$\Delta\epsilon$	$E_c$
	[MPa]	[MPa]	[MPa]	[ $\mu\text{m/m}$ ]	[ $\mu\text{m/m}$ ]	[ $\mu\text{m/m}$ ]	[GPa]
1	2.55	7.64	5.09	133.5	313.3	179.8	28.32
2	2.55	7.64	5.09	149.6	322.8	173.2	29.38
3	2.55	7.64	5.09	137.8	307.5	169.7	30.00
$\bar{x}$						174.2	29.23
$s$						4.19	0.69

**Table 3.** Example  $E_c$  for HPLWC concrete after 3 days after concreting

Sample	$f_c/10$	$f_c/3$	$\Delta\sigma$	$\epsilon_{fc/10}$	$\epsilon_{fc/3}$	$\Delta\epsilon$	$E_c$
	[MPa]	[MPa]	[MPa]	[ $\mu\text{m/m}$ ]	[ $\mu\text{m/m}$ ]	[ $\mu\text{m/m}$ ]	[GPa]
1	2.29	7.12	4.83	232.7	616.6	383.9	12.58
2	2.29	7.12	4.83	224.5	599.6	375.1	12.87
3	2.29	7.12	4.83	221.4	591.2	369.8	13.06
$\bar{x}$						376.3	12.84
$s$						5.82	0.20

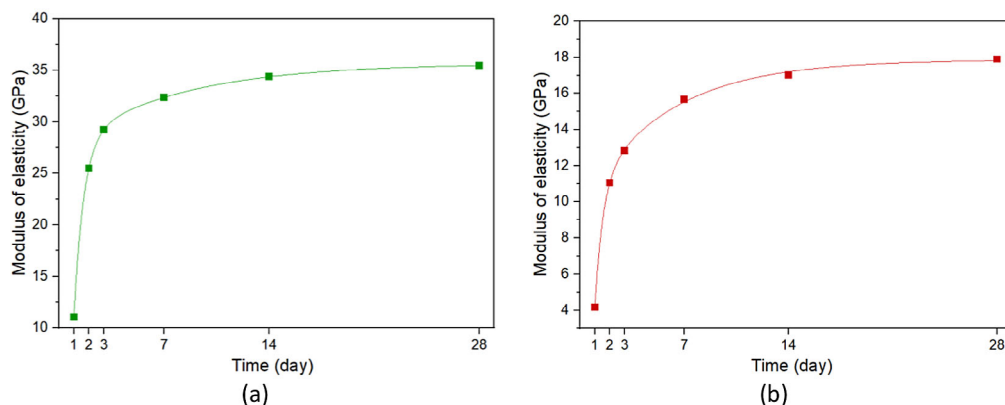


**Figure 8.** Increase in secant modulus of elasticity for the first 28 days: a) C50/60 concrete, b) HPLWC concrete

during the concreting of the bridge structure. Time and transport constraints limited the possibility of taking a larger number of samples. The samples were stored under controlled conditions that ensured adequate humidity and a constant temperature of approximately 20 Celsius degrees during all laboratory tests. The samples were weighed before each test. There were no noticeable changes in the weight of the samples during the tests. So, the moisture saturation level stayed the same during all the tests. Table 4 shows example results for C50/60 concrete 3 days after concreting. Then, according to the procedure described in section 2.4, the frequency of the first axial vibration form was determined, and from it the value of the dynamic modulus of elasticity. Table 5 shows the same data for samples made of HPLWC. It is worth noting the high repeatability and low standard deviation of the obtained results.

In the same way, the  $E_d$  values were determined on each day when measurements were carried out. On Figure 9 shows the change in dynamic modulus of elasticity over the first 28 days. On Figure 9a the results for C50/60 concrete are shown, on Figure 9b for HPLWC. Comparing these 2 diagrams shows a clear difference between

the stiffness of normal and lightweight concrete. As with the secant modulus, the dynamic modulus of lightweight concrete is characterised by half the value of  $E_d$  to normal concrete. It is also worth noting how the stiffness increases. In the case of normal concrete, there was a very noticeable increase in Young's modulus in the first few days after concreting and then a stabilisation of the results. In the case of HPLWC, the increase in stiffness was prolonged over time.

### Comparison of results static and dynamic

Figure 10 shows a comparison of the dynamic and static elastic modulus values of the two tested concretes. In the figure, a significantly different ratio can be observed between the dynamic and static modulus values of the two concretes. To better illustrate this phenomenon in Figure 11 shows the percentage difference between the dynamic and secant modulus of elasticity. In the case of C50/60 concrete, the dynamic modulus obtains significantly higher values from the first days. The difference increases very dynamically in the first few days, then stabilises at around 17%. In the case of HPLWC concrete, the secant modulus

**Table 4.** Example  $E_d$  for C50/60 concrete after 3 days after concreting

Sample	Mass	Density	Frequency	$E_d$
	[g]	[kg/m <sup>3</sup> ]	[Hz]	[GPa]
1	9454	2364	4698	33.39
2	9531	2407	4787	35.29
3	9477	2418	4761	35.07
4	9585	2349	4769	34.19
$\bar{x}$	9512	2384	4754	34.48
s	50.7	28.7	33.2	0.75

**Table 5.** Example  $E_d$  for HPLWC concrete after 3 days after concreting

sample	Mass	Density	Frequency	$E_d$
	[g]	[kg/m <sup>3</sup> ]	[Hz]	[GPa]
1	6636	1659	3505	13.04
2	6597	1666	3515	13.17
3	6458	1647	3534	13.17
4	6675	1636	3525	13.01
5	6772	1676	3537	13.42
6	6588	1664	3541	13.35
7	6725	1681	3526	13.38
$\bar{x}$	6636	1661	3526	13.22
s	95.2	14.6	11.9	0.15



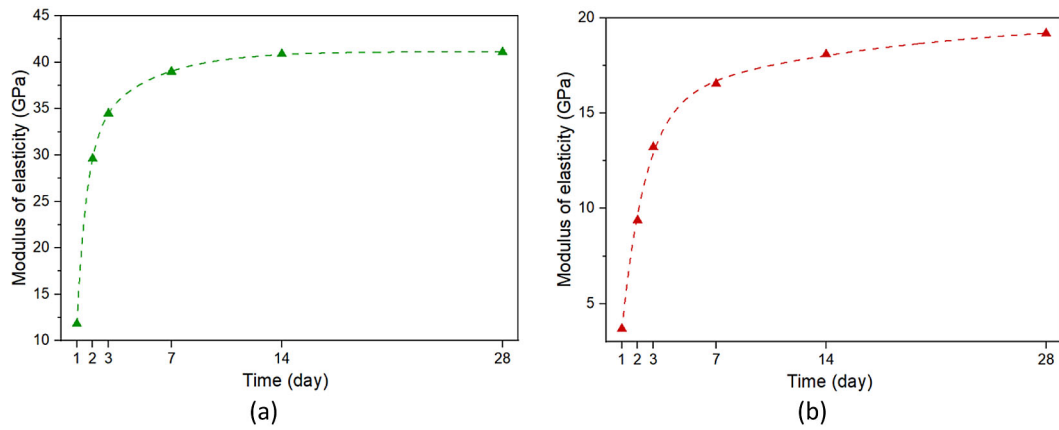


**Figure 9.** Increase in dynamic modulus of elasticity for the first 28 days, (a) C50/60 concrete, (b) HPLWC concrete

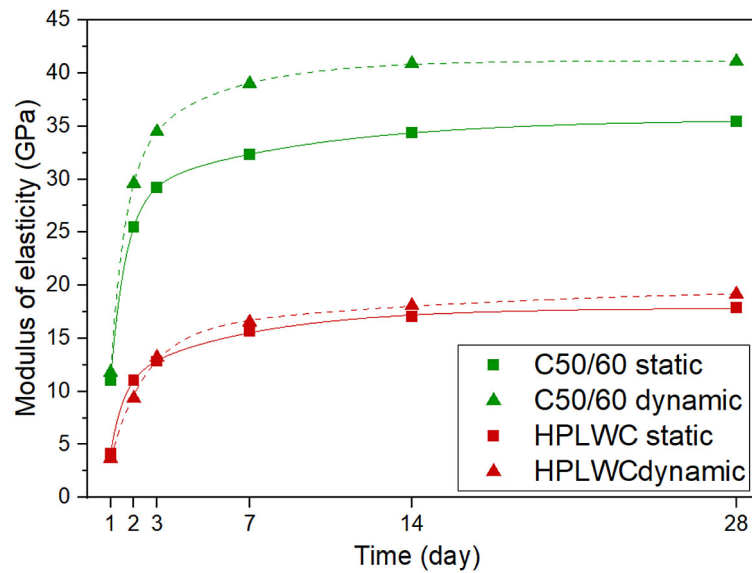


**Figure 10.** Comparison of secant and dynamic modulus of elasticity of two tested concretes

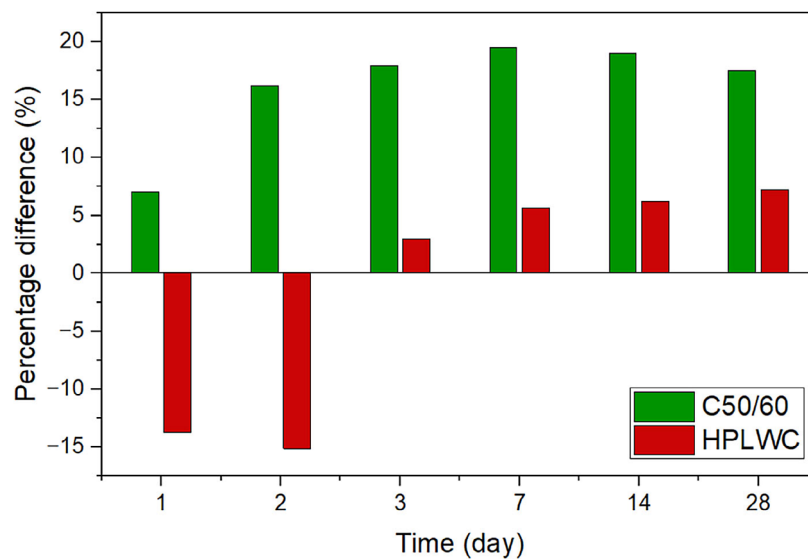


**Figure 11.** Percentage difference between dynamic and secant elastic modulus

is slightly greater than the dynamic modulus in the first few days. Already around the third day, the trend reversed. On the following days, the value of the dynamic module exceeded the static module by only about 5%. At Figure 12 additionally shows the relations between the dynamic and secant modulus of elasticity of concrete and its compressive strength developing within the first 28 days after concreting. It is worth noting that in the case of conventional C50/60 concrete, these relationships are clearly non-linear [23] (Figure 12a). In the case of lightweight concrete (Figure 12b) the relationship is more linear.

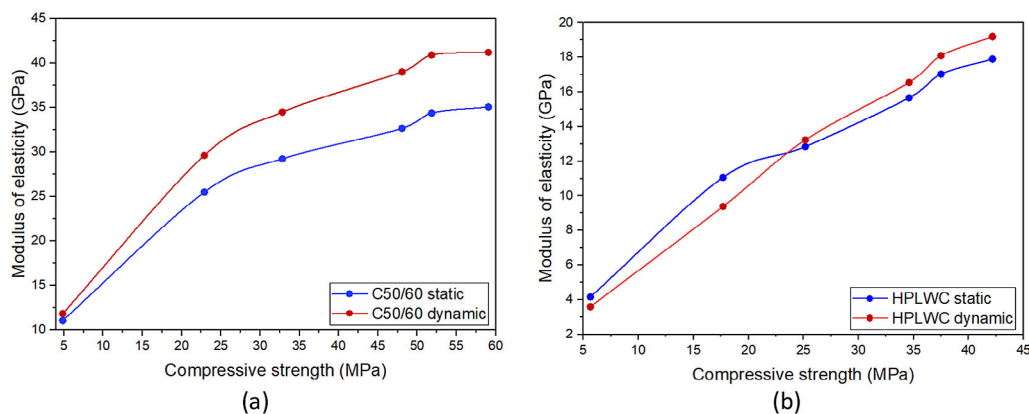
## Discussion

Table 6 shows the values of the ratio of static to dynamic modulus  $E_c/E_d$  determined experimentally for the two tested concretes. These values were compared with those determined according to the literature relations presented in equations (1) to (4). For normal C50/60 concrete, all the equations proposed in the literature agree with the values obtained experimentally in a satisfactory degree. However, for modern HPLWC concrete, the literature values are different from the experimental values, strongly undervaluing it.

The difference in the ratio between the static and dynamic modulus is explained by the fact that normal concretes have more non-linear stress-strain characteristics than lightweight concretes.

This relationship was measured not only over the range required to determine the secant modulus, but over the full load range up to failure. At Figure 13 shows an example of the results. Figure 13a presented relationship for C50/60 after 3 days, a Figure 13b for HPLWC also after 3 days. Figure 13c and d show analogous results obtained after 14 days.

A thorough analysis of the results presented here reveals that ordinary concretes exhibit a higher capacity for plastic deformation. It is evident that the basis of plasticity in concrete is entirely distinct from that observed in metals. It is the consequence of the development of cracks in concrete. However, this phenomenon has the consequence of rendering the non-linear part of the stress-strain relationship well visible. In the case of HPLWC concrete, a far more linear characteristic is apparent. Furthermore, the failure process is characterised by a more fragile nature. This phenomenon is demonstrated in greater detail in Figure 14, which presents a change in Poisson's ratio as a function of load. As illustrated in Figure 14a, there is a discernible increase in the Poisson's ratio at the component's terminal point, which is concomitant with the onset of crack formation within the material. In the case of HPLWC (Figure 14b), this phenomenon does not occur at all, indicating the very brittle and rapid failure mode of this material during compression.



**Figure 12.** Relationship between compressive strength and modulus of elasticity for the first 28 days: (a) C50/60 concrete, (b) HPLWC concrete

**Table 6.**  $E_c/E_d$  ratio determined experimentally and in accordance with the literature

Concrete	$E_c / E_d$				
	Experiment	eq. (1)	eq. (2)	eq. (3)	eq. (4)
C50/60	0.85	0.83	0.79	-	0.82
HPLWC	0.93	0.83	-	0.83	0.84

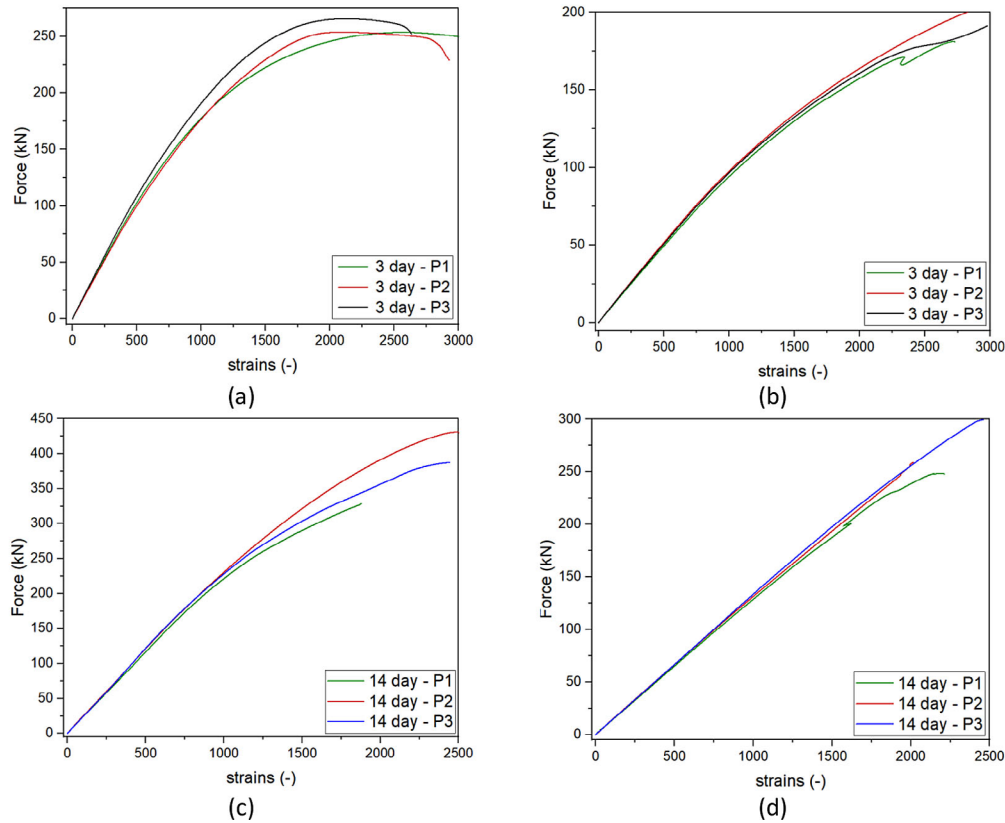


**Figure 13.** Stress-strain relationship of the tested concretes at selected days, (a) C50/60 after 3 days, (b) HPLWC after 3 days, (c) C50/60 after 14 days, (d) HPLWC after 14 days

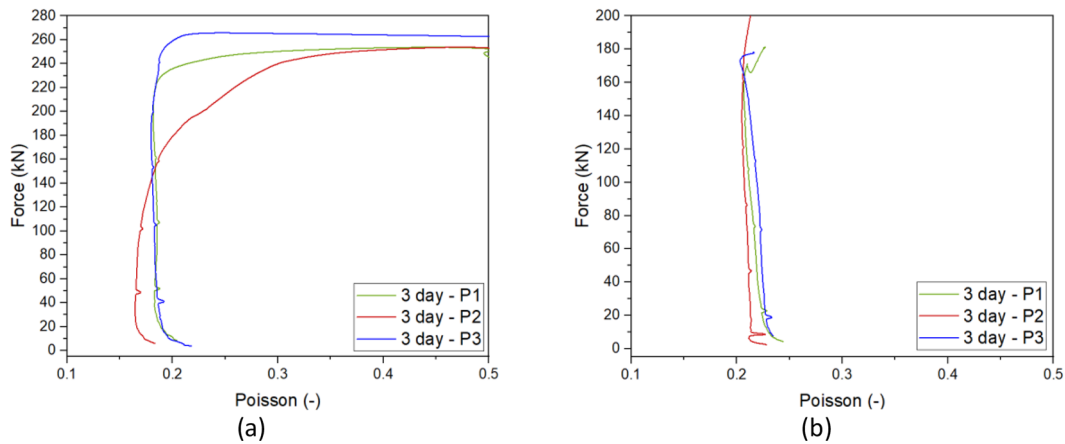


**Figure 14.** Poisson's ratio 3 days after concreting, (a) C50/60 concrete, (b) HPLWC concrete

## CONCLUSIONS

This paper focuses on a fundamental material parameter relevant to the dynamic analysis of structures: the modulus of elasticity. Concrete, as one of the primary materials used in construction, exhibits differing values for its static and dynamic modulus of elasticity. This article explores the underlying causes of this discrepancy. While numerous studies in the literature outline the relationship between

static and dynamic moduli, this ratio in practice depends on several factors, particularly the type and grain size of the aggregate.

In the case of lightweight concrete, the situation is even more complex. Depending on the target density, a wide range of aggregates and production technologies may be employed. The common practice of assuming a generalized modulus ratio in structural modelling [24] further complicates the issue and highlights the need for more targeted research.

This is particularly relevant in the context of modern high-strength lightweight concretes, such as HPWLC. In this study, Liaver-based glass aggregate concrete is used as a case study.

The following conclusions were drawn from the experimental investigation:

- the tested high-strength lightweight concrete exhibited only a small difference between its dynamic and static modulus of elasticity, approximately 5% in hardened state;
- this small discrepancy is advantageous for dynamic structural analysis, as the static modulus may be reliably used for dynamic modelling purposes;
- further studies are necessary to confirm these findings and to establish generalizable conclusions regarding the dynamic properties of modern high-strength lightweight concretes;
- the article presents the results of measurements taken during the first standard 28 days; the authors of the study repeated the entire set of tests two years after concreting. These results will be presented in a publication on the practical application of HPLWC in building structures.

## REFERENCES

1. Jajodia R, Gadve S. Development of statistical model for prediction of modulus of elasticity of concrete. *Structural Concrete* 2023;24:4297–312. <https://doi.org/10.1002/SUCO.202200996>
2. Domagała L, Margańska M, Miazgowiec M. Moisture impact on static and dynamic modulus of elasticity in structural normal-weight concretes. *Materials* 2024;17(15):3722. <https://doi.org/10.3390/ma17153722>
3. Cheng H, Liang M. Real-time monitoring of static elastic modulus evolution in hardening concrete through longitudinal-wave velocity changes retrieved by the stretching technique. *Constr Build Mater* 2024;453:139086. <https://doi.org/10.1016/J.CONBUILDMAT.2024.139086>
4. Bolborea B, Baera C, Dan S, Gruin A, Burduhos-Nergis DD, Vasile V. Concrete compressive strength by means of ultrasonic pulse velocity and moduli of elasticity. *Materials* 2021;14:7018. <https://doi.org/10.3390/MA14227018>
5. Abramowicz M, Berczyński S, Wróblewski T. Parameter estimation of a discrete model of a reinforced concrete slab. *Journal of Theoretical and Applied Mechanics (Poland)* 2017;55:407–20. <https://doi.org/10.15632/JTAM-PL.55.2.407>
6. Del Savio AA, La Torre Esquivel D, Carrillo J, Chi Yep E. Determination of polypropylene fiber-reinforced concrete compressive strength and elasticity modulus via ultrasonic pulse tests. *Applied Sciences* 2022;12:10375. <https://doi.org/10.3390/AP122010375>
7. Thomaz W de A, Miyaji DY, Possan E. Comparative study of dynamic and static Young's modulus of concrete containing basaltic aggregates. *Case Studies in Construction Materials* 2021;15. <https://doi.org/10.1016/j.cscm.2021.e00645>
8. Lin H, Takasu K, Suyama H, Koyamada H, Liu S. A study on properties, static and dynamic elastic modulus of recycled concrete under the influence of modified fly ash. *Constr Build Mater* 2022;347. <https://doi.org/10.1016/j.conbuildmat.2022.128585>
9. Trifone L. A Study of the Correlation Between Static and Dynamic Modulus A Study of the Correlation Between Static and Dynamic Modulus of Elasticity on Different Concrete Mixes of Elasticity on Different Concrete Mixes. 2017.
10. Almeida OML, Diógenes HJF, Melo AA, Almeida OML, Diógenes HJL. Experimental study of the static and dynamic modulus of elasticity of lightweight concrete with the use of expanded clay for structural purposes. *Holos* 2023;3:e14312. <https://doi.org/10.15628/holos.2023.14312>
11. Popovics J. A Study of Static and Dynamic Modulus of Elasticity of Concrete - Final report, American Concrete Institute. 2007.
12. European Committee for Standardization. EN 12390-13:2021 - Testing hardened concrete - Part 13: Determination of secant modulus of elasticity in compression 2021.
13. Lydon FD, Balendran RV. Some observations on elastic properties of plain concrete. *Cem Concr Res* 1986;16:314–24. [https://doi.org/10.1016/0008-8846\(86\)90106-7](https://doi.org/10.1016/0008-8846(86)90106-7)
14. BSI British Standards Institution. BS 8110-2:1985 - Structural use of concrete - Code of practice for special circumstances. BSi British Standard 1985.
15. Swamy R, Bandyopadhyay A. The elastic properties of structural lightweight concrete. *Proceedings of the Institution of Civil Engineers* 2015;59:381–94. <https://doi.org/10.1680/IICEP.1975.3671>
16. Popovics S. Verification of relationships between mechanical properties of concrete-like materials. *Matériaux et Constructions* 1975;8:183–91. <https://doi.org/10.1007/BF02475168/METRICS>
17. European Committee for Standardization. EN 206:2013 - Concrete - Specification, performance, production and conformity 2013.
18. Tahwia AM, Essam A, Tayeh BA, Elrahman MA. Enhancing sustainability of ultra-high performance concrete utilizing high-volume waste



- glass powder. *Case Studies in Construction Materials* 2022;17:e01648. <https://doi.org/10.1016/J.CSCM.2022.E01648>
19. Al-kroom H, Abd Elrahman M, Stephan D, Strzałkowski J, Stolarska A, Chung SY, et al. Physico-mechanical properties, microstructure, and durability of ultra-high-performance lightweight concrete (UHPLWC) incorporating expanded thermoplastic microspheres and basalt fibers. *Constr Build Mater* 2025;494. <https://doi.org/10.1016/j.conbuildmat.2025.142868>
20. Kwang-Myong L, Dong-Soo K, Jee-Sang K. Determination of dynamic Young's modulus of concrete at early ages by impact resonance test. *KSCE Journal of Civil Engineering* 1997;1.
21. ASTM C215-19 - Test Method for Fundamental Transverse, Longitudinal, and Torsional Resonant Frequencies of Concrete Specimens. ASTM International; 2019. <https://doi.org/10.1520/C0215-19>
22. Neville A. M. *Properties of Concrete*. Edition V. Pearson Education Limited; 2011.
23. Jurowski K, Grzeszczyk S. Influence of selected factors on the relationship between the dynamic elastic modulus and compressive strength of concrete. *Materials* 2018;11. <https://doi.org/10.3390/ma11040477>
24. Pelka-Sawenko A, Abramowicz M, Wróblewski T, Berczyński S, Szumigala M. Modeling and analysis of free vibration of steel-concrete composite beams. *Recent Advances in Computational Mechanics - Proceedings of the 20th International Conference on Computer Methods in Mechanics, CMM 2013, 2014*.